

# Self-powered Breath Monitoring using Electrospun Biodegradable and Biocompatible Textile Sensors

Sanjaya D. G. Karnasooriya Ragalage  
Insight SFI Research Centre for Data  
Analytics  
School of Electronic Engineering  
Dublin City University  
Dublin, Ireland  
[Sanjaya.gunawardhana2@mail.dcu.ie](mailto:Sanjaya.gunawardhana2@mail.dcu.ie)

Hamza Qadeer  
Insight SFI Research Centre for Data  
Analytics  
Dublin City University  
Dublin, Ireland  
[Hamza.qadeer@dcu.ie](mailto:Hamza.qadeer@dcu.ie)

Garrett B. McGuinness  
School of Mechanical Engineering  
Dublin City University  
Dublin, Ireland  
[Garrett.mcguinness@dcu.ie](mailto:Garrett.mcguinness@dcu.ie)

Tomas E Ward  
Insight SFI Research Centre for Data  
Analytics  
School of Computing  
Dublin City University  
Dublin, Ireland  
[Tomas.ward@dcu.ie](mailto:Tomas.ward@dcu.ie)

Shirley M. Coyle  
Insight SFI Research Centre for Data  
Analytics  
School of Electronic Engineering  
Dublin City University  
Dublin, Ireland  
[Shirley.coyle@dcu.ie](mailto:Shirley.coyle@dcu.ie)

**Abstract**— This paper presents the development of self-powered breath monitoring sensors using triboelectric nanogenerators (TENGs) technique fabricated from electrospun polycaprolactone (PCL) and cellulose acetate (CA) fibers. The CA was chemically modified with 0.2M NaOH, achieving a maximum open-circuit voltage ( $V_{oc}$ ) of 14.3 V, short-circuit current ( $I_{sc}$ ) of 1.67  $\mu$ A and charge ( $Q_{sc}$ ) of 6.61 nC. Incorporating 3% chitosan into PCL further enhanced the sensor's performance, yielding a  $V_{oc}$  of 20.8 V,  $I_{sc}$  of 3.178  $\mu$ A, and  $Q_{sc}$  of 9.9 nC. The sensor demonstrated excellent sensitivity, with a linear response and a sensitivity of 2.209 V/kPa across a pressure range of 0.625-12.5 kPa. It also exhibited rapid response times of 34-36 ms and recovery times of 24-26 ms. The optimized materials and sensor configuration show promise for continuous real-time breath monitoring. This innovation provides a significant advancement in wearable health monitoring systems, enabling early detection of respiratory illnesses and chronic disease management.

**Keywords**—Self-powered Sensors, Smart Textiles Electrospinning, Breath Monitoring, Biodegradable

## I. INTRODUCTION

The development of self-powered sensors for health monitoring is a significant advancement in wearable technology. These sensors enable continuous real-time tracking of physiological signals without external power sources. Breath monitoring sensors are particularly crucial, providing vital respiratory health information, early detection of diseases, and monitoring overall wellness[1].

Shen et al. highlighted the use of TENGs for continuous breath monitoring, eliminating the need for batteries. TENGs operate on the principle of the triboelectric effect and electrostatic induction between different materials[1]. Wang et al. developed a breath monitoring TENG sensor using polytetrafluoroethylene and Cu wire as the triboelectric materials, which could detect slow, rapid, shallow and deep breathing patterns accurately[2]. While in previous literature, nonbiodegradable polymeric materials are prominently used, recently, there has been a trend to use biodegradable and biocompatible polymers in wearable sensors[3]. PCL and CA are two promising materials for fabricating wearable textile sensors due to their biocompatibility, flexibility, and ease of fabrication through electrospinning. Electrospun PCL and CA fibers offer a high surface area-to-volume ratio, essential for

enhancing the sensitivity and efficiency of breath monitoring sensors[4].

In this study, for the first time we explore the potential of electrospun PCL and CA fibers for use in self-powered breath monitoring sensors. Specifically, we investigate the effects of modifying CA by deacetylation with NaOH at concentrations ranging from 0.05M to 0.25M and combining PCL with 3% chitosan (Fig. 1a). Our results demonstrate that CA modified with 0.2M NaOH and PCL combined with chitosan exhibit significantly improved performance in TENGs, which serve as self-powered sensors for breath monitoring.

Final sensor samples were attached to conductive fabrics and affixed to a face mask using paper brackets (Fig. 1b). The sensor successfully identified a range of simulated breathing patterns, demonstrating the feasibility of this technique for future wearable self-powered sensors. This research highlights the importance of material modifications in enhancing the functionality and efficiency of self-powered sensors. By optimizing electrospinning conditions and material compositions, we aim to advance the development of highly sensitive, reliable, and sustainable breath monitoring devices that can be integrated into wearable health monitoring systems. Future work may further enhance these technologies with signal processing and AI techniques for continuous breath monitoring.

## II. MATERIALS AND METHOD

### A. CA Electrospinning

CA (molecular weight (MW) 30,000, Sigma-Aldrich®), acetone, and N, N-Dimethylformamide (DMF) were procured and utilized as received for the preparation of the CA precursor. A quantity of 2.5 g of CA was dissolved in a 10 g solution of DMF: Acetone (2:3 ratio), and the mixture was magnetically stirred for 4 hours at room temperature. The solution was loaded into a syringe with a 20 G blunt needle for electrospinning at a flow rate of 2 mL/h, with a 15 cm tip-to-collector distance and 15 kV applied voltage for 1.5 hours. The electrospun membrane was collected on aluminum foil attached to a rotating mandrel (2000 rpm), then dried and annealed at 200 °C for 1 hour. (Fig 1a). NaOH solutions (0.05M to 0.25M in 0.05M increments) were prepared, and dried CA samples were cut, immersed in these solutions for 30 minutes, then thoroughly washed with deionized water and dried in a fume hood for 24 hours.

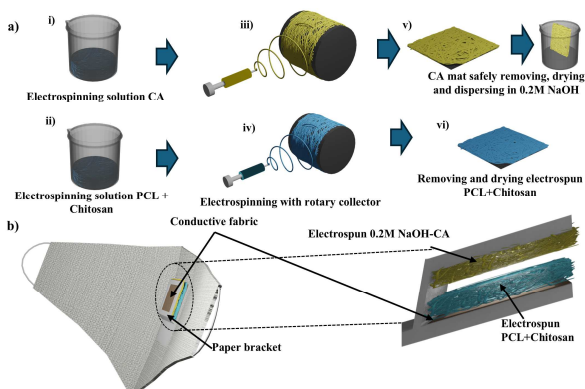


Fig. 1. Device fabrication process a) Electrospinning sample preparation: i) CA and ii) PCL + chitosan precursor preparation, iii) and iv) Electrospinning process, v) Deacetylation of CA with NaOH and drying of all samples, vi) Removal from aluminum foil and drying of PCL + chitosan samples., b) Final prototype sensor attached to the fabric mask.

### B. PCL Electrospinning

PCL (MW 80,000, Sigma-Aldrich®), Formic, and Acetic acid were acquired and used as received for the preparation of the PCL precursor. 1.9 g of PCL was dissolved in a 1:1 ratio of 10 g Formic acid and Acetic acid solution and stirred magnetically for 8 hours at 50°C to completely dissolve the PCL pellets. The solution was loaded into a syringe with a 20 G blunt needle for electrospinning at a flow rate of 2 mL/h, 11 cm tip-to-collector distance, and 16 kV applied voltage for 1 hour. The membrane was collected in the same manner as the CA and delicately removed from the aluminum foil, then dried in a fume hood for 24 hours prior to characterization.

For the second trial, Chitosan (medium MW, Sigma-Aldrich®) was procured and used in conjunction with the PCL precursor. The PCL precursor was prepared as previously described, and 0.3 g of Chitosan was mixed with 10 g of precursor and stirred thoroughly for 2 hours. After dissolution, electrospinning was carried out using the same procedure employed for PCL and dried for 24 hours before the subsequent process.

### C. Material Characterization

The samples underwent Scanning Electron Microscopic (SEM) imaging with a Jeol JSM-IT 100 InTouchScope SEM, and Fourier-transform infrared spectroscopy (FTIR) was conducted using a PerkinElmer Spectrum Two FT-IR.

### D. Self-powered Sensor Performance

CA and PCL samples were cut into 16 cm<sup>2</sup> pieces for electrical characterisations and affixed to two copper plates using 3M 9713XYZ tape. The copper plates were then secured to Perspex sheets to facilitate contact and separation motion between the samples, and the applied force was measured using an attached load cell.  $V_{OC}$  was measured with a Tektronix TBS 1052B-EDU digital oscilloscope.  $I_{SC}$  and  $Q_{SC}$  were measured using a Keithley 6517B electrometer.

## III. RESULTS

### A. Morphology and Chemical Modifications

SEM images of CA (Fig. 2a) and NaOH-treated cellulose acetate (NaOH-CA) (Fig. 2b) demonstrate that the fibers retain a similar alignment post-treatment. However, there is a significant increase in the average fiber diameter, from 0.615  $\mu\text{m}$  in CA to 1.208  $\mu\text{m}$  in NaOH-CA. This increase in diameter is attributed to the deacetylation process, where the

treatment with NaOH converts cellulose acetate into cellulose II. This chemical transformation promotes fiber swelling and leads to the development of a rougher and more porous fiber surface. These morphological changes are indicative of the removal of acetyl groups and the consequent exposure of hydroxyl groups, enhancing the porosity of the fibers.

The SEM image of PCL (Fig. 2c) reveals a substantial enhancement in surface area due to the formation of a micro- and nanofiber web. The fibers exhibit an average diameter of 0.501  $\mu\text{m}$ , with branching nanofibers further increasing the surface area. This intricate network structure is advantageous for TENG, as the increased surface area can enhance charge generation and storage capabilities. When PCL is combined with chitosan, the average fiber diameter increases to 0.770  $\mu\text{m}$ , and the fibers exhibit a more pronounced alignment in a single direction compared to PCL alone (Fig 2d). This enhanced alignment may improve the consistency and efficiency of charge transfer, making the composite material particularly suitable for high-performance TENGs.

Analysis of the FTIR spectra of CA and NaOH-CA reveals significant changes (Fig 2e). The absorption peak at 1739  $\text{cm}^{-1}$ , associated with C=O stretching, and the peak at 1365  $\text{cm}^{-1}$ , corresponding to C-H stretching, show a clear reduction after treatment. Furthermore, peaks related to C-O stretching (1050-1150  $\text{cm}^{-1}$ ) and O-H stretching (3400-3500  $\text{cm}^{-1}$ ) are prominently visible in the treated sample, indicating successful deacetylation[5].

The FTIR spectra of the PCL/chitosan blend show decreased peak intensities compared to pure PCL (Fig 2f). The interaction between the carbonyl groups of PCL and the amino groups of chitosan has reduced the peak intensity at 1723  $\text{cm}^{-1}$ , while the interaction between the ester groups of PCL and chitosan has also reduced the peak at 1295  $\text{cm}^{-1}$ .

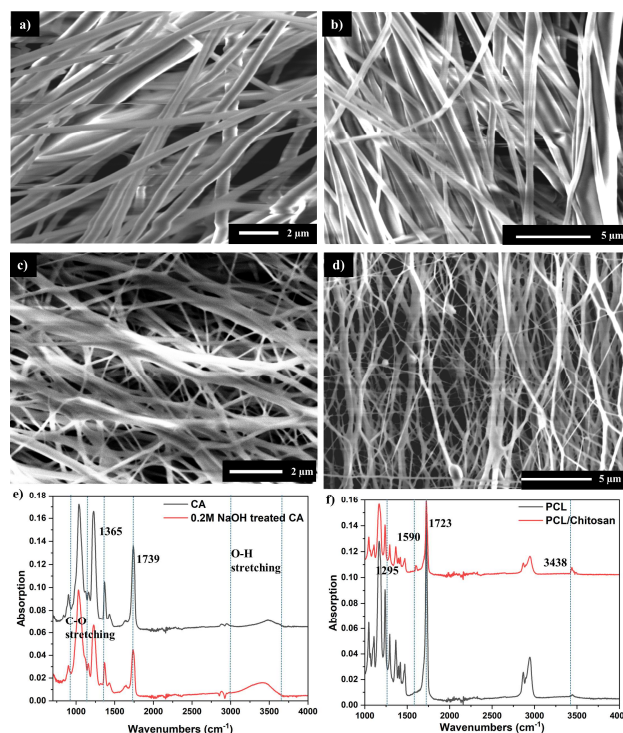


Fig. 2. SEM and FTIR analysis. SEM images of a) CA, b) 0.2M NaOH-CA, c) PCL and d) PCL/Chitosan, FTIR analysis of e) CA and 0.2M NaOH-CA, f) PCL and PCL/chitosan.

The peak at  $3438\text{ cm}^{-1}$ , associated with hydrogen bonding, has broadened and become more pronounced, indicating an interaction between the hydroxyl groups of PCL and the amino groups of chitosan. Additionally, a new peak at  $1590\text{ cm}^{-1}$ , characteristic of the PCL/chitosan blend, has appeared, demonstrating the effective blending of PCL and chitosan in the composite electrospun structure[6].

### B. Self-powered Sensor Performance

Initially, all NaOH-CA samples were subjected to contact and separation motion with the PCL sample. 10 N continuous contact and separation was applied at 2 Hz frequency with 5 mm amplitude. The corresponding results are shown in Fig. 3a, b, and c. The average  $V_{OC}$  peak-to-peak values increased with NaOH concentration, peaking at 14.3 V for the 0.2M NaOH-CA sample. Similarly, the highest  $I_{SC}$  and  $Q_{SC}$  were recorded for the 0.2M NaOH-CA sample, at  $1.67\text{ }\mu\text{A}$  and  $6.61\text{ nC}$ , respectively. Conversely, the lowest values were observed for the CA only sample, with a  $V_{OC}$  of 4.87 V,  $I_{SC}$  of  $80.4\text{ nA}$  and a  $Q_{SC}$  of  $1.5\text{ nC}$ .

As we observed in the FTIR spectra acetyl groups are substituted with hydroxyl groups. The introduction of hydroxyl groups in treated CA samples promotes hydrogen bonding and other interactions, enhancing the propensity to lose electrons and acquire a more positive charge compared to PCL[3]. Furthermore, the thickness of the samples has slightly reduced from  $63\text{ }\mu\text{m}$  to  $57\text{ }\mu\text{m}$ , creating a more favourable environment for charge transfer. On the other hand, the swelling of fibers increases the gap between fibers and reduces the surface area. This might cause a reduction in electrical performance after a certain level of deacetylation. Further experiments are required to fully understand this phenomenon.

After achieving peak performance with NaOH modification, another set of experiments was conducted to

modify the PCL. Incorporating chitosan resulted in significant improvements, with  $V_{OC}$  reaching  $20.8\text{ V}$ ,  $I_{SC}$  at  $3.178\text{ }\mu\text{A}$ , and  $Q_{SC}$  at  $9.9\text{ nC}$  (Figure 3 d, e, f). Although adding chitosan did not chemically alter the tribonegative properties of the PCL layer, it significantly modified the surface structure. The more textured surface with aligned fibers increased the surface area, leading to a higher charge density than pure PCL samples. Additionally, the thickness of the samples was significantly reduced from  $55\text{ }\mu\text{m}$  to  $34\text{ }\mu\text{m}$  (for the same electrospinning time), enhancing charge transfer and overall output[4]. This research has explored the feasibility of incorporating chitosan into PCL to improve output performance. Furthermore, the literature suggests that adding chitosan to the PCL network enhances biodegradability, offering the potential to develop sustainable devices[3,6].

As shown in Figure 4a, during breathing, the contact and separation motions between the CA and PCL layers result in an alternating current/voltage output through the external load. This output can be used as the primary signal for determining breath patterns based on these experiments. The variation in current, corresponding to the cyclical motion of the layers, directly reflects the inhalation and exhalation phases, providing a reliable metric for analyzing respiratory activity.

### C. Sensitivity

A series of experiments were conducted to evaluate the sensor's sensitivity for breath monitoring applications and determine the response to applied force, response time, and recovery time. As illustrated in Figure 4b, the sensor exhibited a peak-to-peak voltage of  $9.56\text{ V}$  at an applied force of  $1\text{ N}$ , with a maximum voltage of  $34.6\text{ V}$  achieved at  $20\text{ N}$ . Additionally, the device demonstrated a linear response ( $R^2 = 0.986$ ) with a sensitivity of  $2.209\text{ V/kPa}$  over a pressure range of  $0.625\text{--}12.5\text{ kPa}$  (Fig 4c).

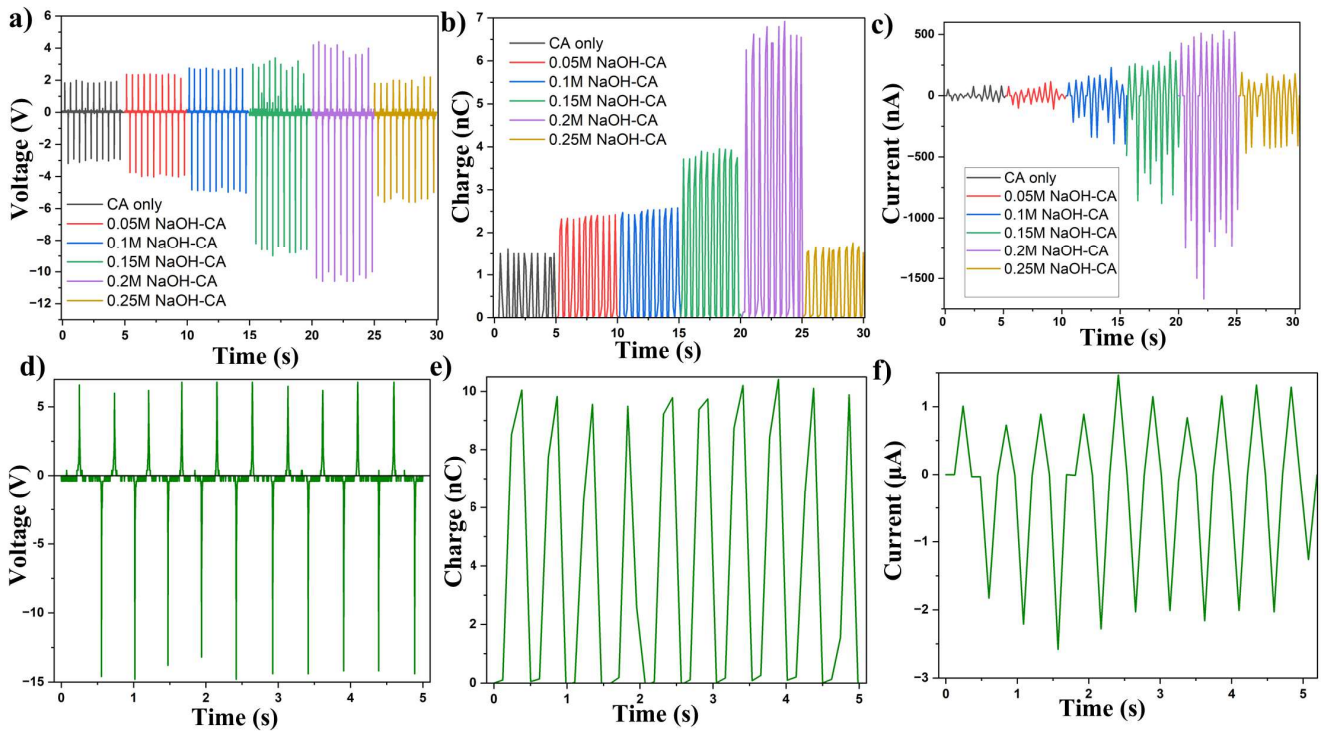


Fig. 3. Triboelectric performance of developed samples. Change of voltage (a), charge (b) and current (c) performance with the chemical modification of CA with NaOH., Output performance voltage (d), charge (e) and current (f) when 0.2M NaOH-CA sample contact and separated with PCL/chitosan composite electrospun sample.

#### IV. DISCUSSION

The device characteristics demonstrate the feasibility of this approach for monitoring breathing signals.

Normal breathing rates range from 12 to 20 breaths per minute. Rates above this range indicate tachypnea, characterized by rapid breathing, while rates below suggest bradypnea, characterized by slow breathing. Detecting apnea, marked by the cessation of breathing, is crucial and requires high sensitivity to low pressures[7]. The sensor's response time was recorded as 34 ms to reach any given positive peak at 1N force and 36 ms at 40 N force. Recovery times were 24 ms for 1N force and 26 ms for 40 N force (Fig 4d). These results indicate that the sensor is well-suited for continuous respiratory rate monitoring and is capable of detecting changes in respiration over time.

To demonstrate the feasibility of this application, the sensor was integrated into a facemask and evaluated using a model test rig, which consisted of a mannequin head with an air outlet at the mouth attached by tubing to a manual air pump. The mask was placed on the face of the mannequin head in front of the air outlet, and different breathing patterns were simulated by controlling the airflow via the manual pump. The sensor was capable of distinguishing different signal features with slow, rapid, deep slow, and deep rapid breathing patterns, as shown in Fig 4e. Biocompatibility for long-term exposure and a feasible wireless signal detection technique need to be developed before conducting experiments with human participants.

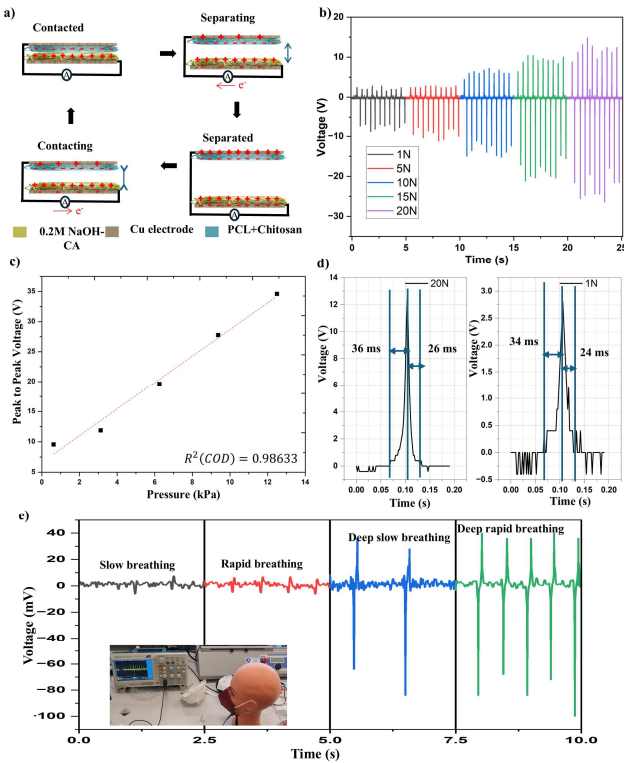


Fig. 4. Sensitivity performance analysis and application development. a) The working principle of the triboelectric breath monitoring sensor. b) Voltage output change with different applied force, c) Linear relationship between the voltage and pressure, d) Response and recovery time measurement for 20 N and 1 N applied force., e) Voltage response with slow, rapid, deep slow and deep rapid breathing patterns.

#### V. CONCLUSION

In this study, we developed a high-performance breath monitoring sensor by incorporating chitosan into PCL and chemically modifying CA with NaOH. The results demonstrate that NaOH modification significantly enhanced the triboelectric performance of CA, with the 0.2M NaOH-CA sample achieving the highest outputs  $V_{OC}$  of 14.3 V,  $I_{SC}$  of 1.67  $\mu$ A, and  $Q_{SC}$  of 6.61 nC. Subsequent incorporation of chitosan into PCL further improved the sensor's performance. The PCL/chitosan blend showed enhanced  $V_{OC}$  of 20.8 V,  $I_{SC}$  of 3.178  $\mu$ A, and  $Q_{SC}$  of 9.9 nC. Although chitosan did not chemically alter the tribonegative properties of the PCL layer, it significantly modified the surface structure, increasing the texture and alignment of fibers, which contributed to a higher charge density and improved overall output. The sensor exhibited excellent sensitivity with linear response ( $R^2 = 0.986$ ) with a sensitivity of 2.209 V/kPa across a pressure range of 0.625-12.5 kPa. The response time was recorded as 34 ms for lower forces and 36 ms for higher forces, while recovery times were 24 ms and 26 ms, respectively. These findings confirm the feasibility of incorporating chitosan into PCL and chemically modifying CA to enhance TENG performance for respiratory monitoring. Additionally, chitosan improves PCL biodegradability, supporting sustainable device development. Future work will optimize composition and investigate long-term stability and biodegradability to advance eco-friendly sensors.

#### ACKNOWLEDGMENT

The authors acknowledge the funding and support given by Insight SFI Research Centre for Data Analytics in Dublin City University (SFI/12/RC/2289\_P2). The SEM was carried out at the NRF in Dublin City University which was funded under the PRTL Cycle 5. The PRTL is co-funded through the European Regional Development Fund, part of the European Union Structural Funds Programme 2011–2015.

#### REFERENCES

- [1] Shen S, Xiao X, Xiao X, Chen J. Triboelectric Nanogenerators for Self-Powered Breath Monitoring. *ACS Appl Energy Mater* 2022;5:3952–65. <https://doi.org/10.1021/acsaem.1c02465>.
- [2] Wang M, Zhang J, Tang Y, Li J, Zhang B, Liang E, et al. Air-Flow-Driven Triboelectric Nanogenerators for Self-Powered Real-Time Respiratory Monitoring. *ACS Nano* 2018;12:6156–62. <https://doi.org/10.1021/acsnano.8b02562>.
- [3] Meng H, Yu Q, Liu Z, Gai Y, Xue J, Bai Y, et al. Triboelectric performances of biodegradable polymers. *Matter* 2023;6:4274–90. <https://doi.org/10.1016/j.matt.2023.09.017>.
- [4] Gunawardhana KRS, Simorangkir RBVB, McGuinness GB, Rasel MS, Colorado LAM, Baberwal SS, et al. The Potential of Electrospinning to Enable the Realization of Energy-Autonomous Wearable Sensing Systems. *ACS Nano* 2024;18:2649–84. <https://doi.org/10.1021/ACS.NANO.3C09077>.
- [5] Song J, Birbach NL, Hinestroza JP. Deposition of silver nanoparticles on cellulosic fibers via stabilization of carboxymethyl groups. *Cellulose* 2012;19:411–24. <https://doi.org/10.1007/s10570-011-9647-3>.
- [6] Van der Schueren L, Steyaert I, De Schoenmaker B, De Clerck K. Polycaprolactone/chitosan blend nanofibres electrospun from an acetic acid/formic acid solvent system. *Carbohydr Polym* 2012;88:1221–6. <https://doi.org/10.1016/j.carbpol.2012.01.085>.
- [7] Ali M, Elsayed A, Mendez A, Savaria Y, Sawan M. Contact and Remote Breathing Rate Monitoring Techniques: A Review. *IEEE Sens J* 2021;21:14569–86. <https://doi.org/10.1109/JSEN.2021.3072607>.